The electronic supplementary information for

Designing an alkali-metal-like superatom Ca_3B for ambient nitrogen reduction to ammonia

Xiao-Ling Zhang,[a,b] Ya-Ling Ye,[a,b] Li Zhang,[a,b] Xiang-Hui Li,[c] Dan Yu,[d] Jing-Hua Chen,[b] and Wei-Ming Sun*[a,b]

[a]*Department of Basic Chemistry, The School of Pharmacy, Fujian Medical University, Fuzhou 350108, People's Republic of China. E-mail: sunwm@fjmu.edu.cn*

[b]*Fujian Key Laboratory of Drug Target Discovery and Structural and Functional Research, The School of Pharmacy, Fujian Medical University, Fuzhou 350108, People's Republic of China.*

[c]*The School of Medical Technology and Engineering, Fujian Medical University, Fuzhou 350004, Fujian, People's Republic of China*

[d]*Laboratory of Theoretical and Computational Chemistry, Institute of Theoretical Chemistry, Jilin University, Changchun 130023, People's Republic of China.*

Table of Contents

1. Tables

Table S1 The HOMO-LUMO gaps for α-spin and β-spin states (Gap_α and Gap_β, in eV) of the most stable Ca_3B cluster calculated by using CAM-B3LYP, LC-BLYP, and M06-2X methods in conjunction with the 6-311+G(3df) basis set.

Isomers	CAM-B3LYP	LC-BLYP	M06-2X
Gap_α	3.27	4.63	2.72
Gap_β	4.35	4.90	3.27

Table S2. The calculated vertical ionization energies (VIEs, in eV) at the CCSD(T)//PBE0/6-311+G(3df) level and NPA charges on boron atom (Q_B, |e|) of M_3B (M = Be and Mg) at the PBE0/6-311+G(3df) level.

Species	VIE	Q_B
Be_3B	6.91	-1.045
Mg_3B	5.19	-1.855

Table S3. The change in NPA charges (ΔQ, |e|) on Ca_3, B atom, and N_2 subunits before and after the N_2 adsorption to Ca_3B at the PBE0/6-311+G(3df) level, where $\Delta Q = Q_{after} - Q_{before}$.

Subunits	Before N_2 adsorption	After N_2 adsorption	ΔQ
Ca_3	2.198	2.182	-0.016
B	-2.198	-0.389	1.809
N_2	0.000	-1.793	-1.793

2. Figures

Fig. S1. Optimized structure of Ca_3B^+ with relative bond lengths, NPA charges, symmetry, and selected bond angle at the PBE0/6-311+G(3df) level.

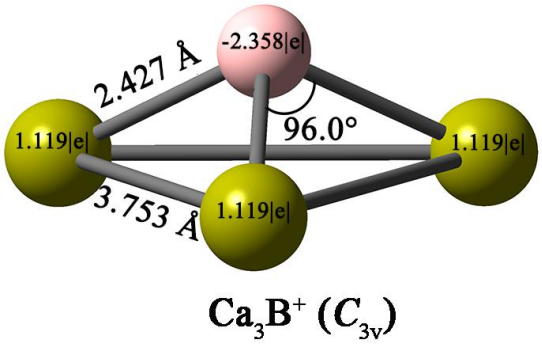

Fig. S2. Global minima of the Mg_3B and Be_3B with selected bond lengths, bond angles, and symmetries at the PBE0/6-311+G(3df) level.

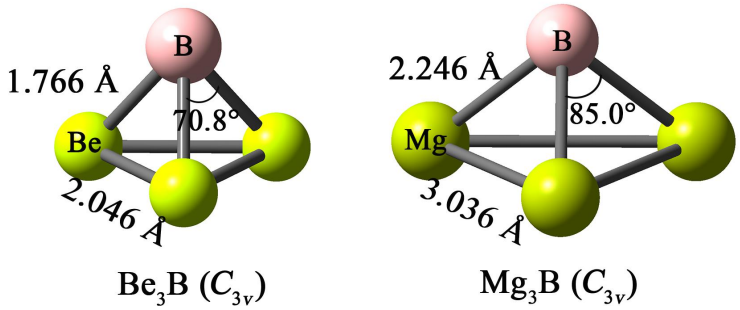

Be_3B (C_{3v}) Mg_3B (C_{3v})

Fig. S3. The relationship between VIE values of M_3B and NPA charges on boron atom (Q_B) as atomic number of alkaline-earth ligand increases.

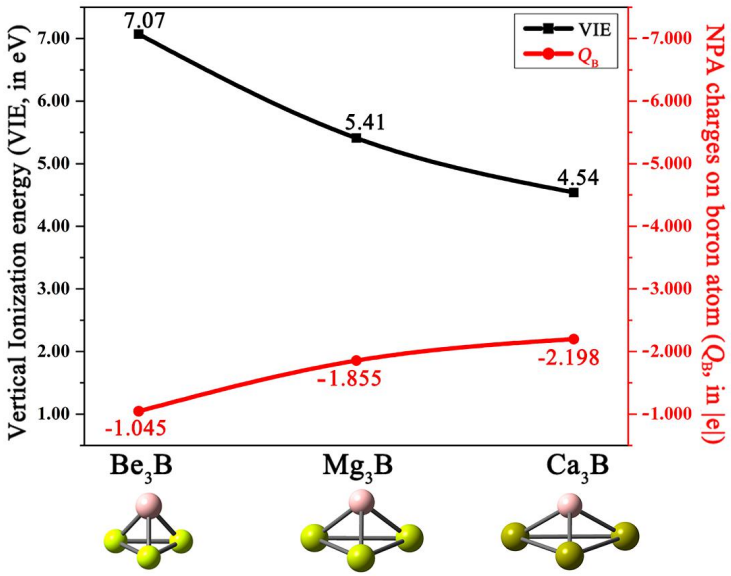

Fig. S4. The optimized structures, selected bond lengths, symmetries, and relative energies (E_{rel}, in kcal/mol) of low-lying Ca_3B-N_2 isomers at the PBE0/6-311+G(3df) level.

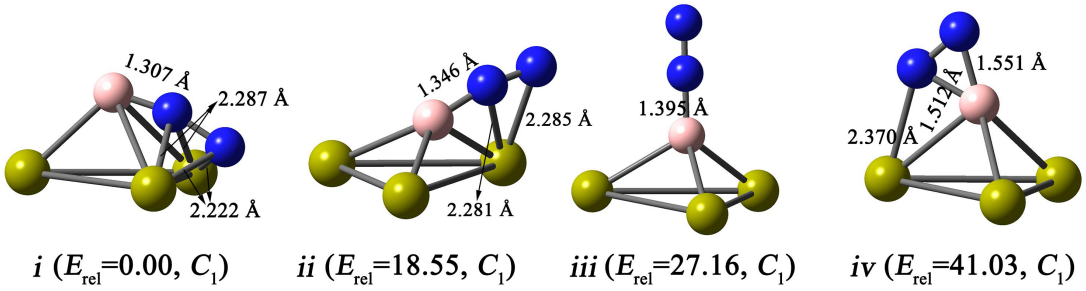

i (E_{rel}=0.00, C_1) *ii* (E_{rel}=18.55, C_1) *iii* (E_{rel}=27.16, C_1) *iv* (E_{rel}=41.03, C_1)

Fig. S5. The optimized structures and N-N bond distance of N_2, diazene (HN=NH), and azobenzene (PhN=NPh) at the PBE0/6-311+G(3df) level.

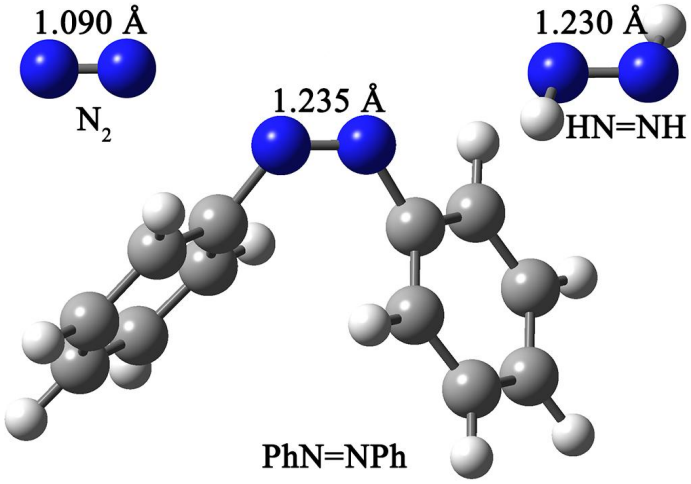

Fig. S6. The optimized structures, selected bond lengths, and adsorption energies (ΔE) for NNH* complex, where $\Delta E = E(\mathrm{NNH^*}) - E(\mathrm{N_2^*}) - E(\mathrm{H^+}) - E(\mathrm{e^-})$.

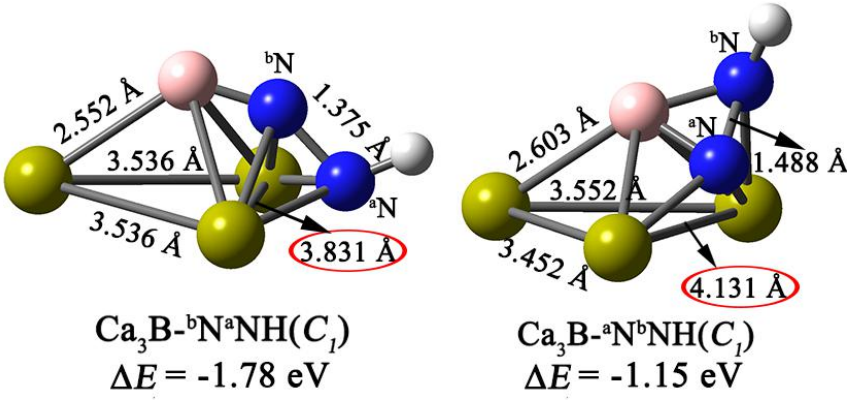

Fig. S7. The variation of N-N distance of critical intermediates in the NRR process of Ca_3B.